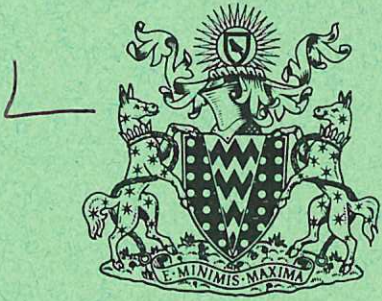
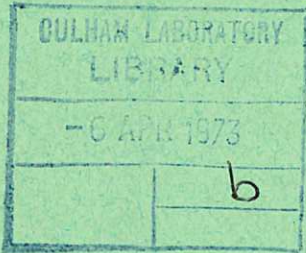


This document is intended for publication in a journal, and is made available on the understanding that extracts or references will not be published prior to publication of the original, without the consent of the authors.



UKAEA RESEARCH GROUP

Preprint

LABORATORY OBSERVATION OF SLOW MODE SHOCK WAVES

A D CRAIG
J W M PAUL

CULHAM LABORATORY
Abingdon Berkshire

1973

Enquiries about copyright and reproduction should be addressed to the Librarian, UKAEA, Culham Laboratory, Abingdon, Berkshire, England

LABORATORY OBSERVATION OF SLOW MODE SHOCK WAVES

A. D. Craig* and J. W. M. Paul

ABSTRACT

We have identified a slow mode shock wave in a laboratory experiment. We also present a model of the novel method of launching the shock.

* Liverpool University

UKAEA Research Group
Culham Laboratory
Abingdon
Berks

January 1973

There have been many reports of laboratory experiments which produce fast mode shock waves propagating into plasmas containing magnetic fields of various magnitudes and directions¹⁻³. Such shocks are associated with the steepening of fast mode MHD waves. Slow mode MHD waves can also, in principle, steepen into shock waves⁴. Space observations^{5,6} have revealed discontinuities in the solar wind which satisfy the conservation relations for such slow shocks. We present here what we believe to be the first laboratory observation of slow mode shock waves.

SLOW MODE SHOCKS

The main differences between fast and slow shocks are described by Kantrowitz and Petschek⁴. Density increases across both, but the transverse component of magnetic field increases across fast and decreases across slow shocks. Thus in slow shocks both magnetic and kinetic energy are converted into thermal energy and it is the thermal pressure

which drives the shock against the magnetic back pressure.

The velocities of flow into (u_1) and out of ($u_2 < u_1$) a slow shock, in its frame of reference, are related to the slow (c_s), intermediate (c_i) and fast (c_f) sound speeds in front (1) and behind (2) as follows:-

$$(i) \ c_{s1} < u_1 < c_{i1} < c_{f1}; \quad (ii) \ u_2 < c_{s2} \leq c_{i2} \leq c_{f2} .$$

METHOD OF LAUNCHING - Ideal MHD Model

In the experiment (Fig.1) we have an annular initial plasma with axial (B_{z0}) and azimuthal ($B_{\theta 0}$) components of magnetic field. The azimuthal, that is transverse, component B_{θ} is decreased at the end insulator by applying a radial electric field (E_r) which drives radial currents.

In discussing the novel principle by which our slow shock is formed, we neglect the cylindrical geometry, but label the Cartesian coordinates r, θ, z for comparison with the experiment.

When the transverse component B_{θ} at the end insulating boundary ($z = 0$) is decreased, a fast expansion wave is launched along the plasma column. For an ideal MHD plasma this will cause plasma to flow towards the insulator. This flow will, by conservation of mass, launch a compressive wave from the insulator and this can steepen into a shock. In order to satisfy the boundary condition, in particular the decrease of transverse component B_{θ} , this must be a slow shock.

We have made this model quantitative by computing the flow through the expansion wave and using the slow shock conservation relations. Fig.2a shows a flow pattern for typical experimental conditions with $B_\theta = 0$ at the end insulator. This forms the so-called 'switch-off' shock.

PISTON FORMATION

Such a flow pattern is not observed in the experiment but this fact can be explained by extending the above model to include a non-idea MHD effect. We assumed above that the transverse component of velocity V_ρ behind the slow shock persists right up to the end insulator. It is this motion which cancels E_r ,

$$\bar{E}_r + \bar{V}_\theta \times \bar{B}_z = 0 ,$$

and prevents radial current flow in the bulk of the plasma.

In practice the end insulator must impose boundary conditions not only $V_z = 0$ but also $V_\theta = 0$. In a real plasma there must, therefore, be a viscous layer to match the transverse velocity of the plasma to the stationary boundary. Because E_r is no longer cancelled, radial current will flow in the layer. The force on this current, $J_r \times B_\theta$, is directed towards the end insulator for $B_\theta \geq 0$ and so the layer does not propagate. The change of B_θ across the layer weakens both the shock and the expansion wave.

If, on the other hand, B_θ reverses at the boundary, then

the force $J_r \times B_\theta$ drives the viscous layer away from the insulator thus forming a piston. The insulator is now in a vacuum and the plasma boundary conditions are effectively transferred to the piston which has both V_z and V_θ components of velocity.

Having introduced this new piston phenomenon from non-ideal MHD, we can now return to our ideal MHD model but include the piston as a discontinuity with specified axial velocity. Using the same method as for Fig.2a we have computed flow patterns, such as Fig.2b, for conditions relevant to the experiment.

One of these conditions is that the piston velocity $V_p < c_{fl}$. This ensures that the piston cannot overtake the fast expansion wave, and then drive a fast shock.

THE APPARATUS (Fig.1)

The discharge chamber, consisting of a Pyrex glass cylinder 1.2 m long and 0.46 m diameter, is immersed in a uniform axial magnetic field $B_{z0} \leq 0.2$ Tesla. A hydrogen plasma is formed by a high current discharge between electrodes A and B. Then an azimuthal magnetic field B_θ is diffused into this plasma by passing a current through the central rod C. After 350 μ s from the initiation of the discharge, a quiescent initial plasma exists with electron density $n_{e0} \sim 5 \times 10^{20} \text{ m}^{-3}$, temperature $T_{e0} \sim 1.3 \text{ eV}$ and $B_{\theta0} \propto 1/r$.

The main experiment involves reducing, cancelling or reversing the B_θ field at the end insulator D by passing a radial current between the ring electrode A and the long centre electrode E. This current rises in $0.5 \mu\text{s}$ and remains constant for $3 \mu\text{s}$.

A more detailed description of the apparatus, but without the facility for $B_{\theta 0}$, is given in an earlier paper² on 'switch-on' shocks.

OBSERVATIONS

The flow patterns are deduced from measurements of the magnetic field B_θ , and hence the current J_r , made by small (~ 2.5 mm) magnetic probes inserted through electrode B.

When B_θ is reduced or cancelled at the insulator, the current remains near the insulator and nothing is observed to propagate. This can be explained by assuming that the radial current in the viscous layer so weakens the expansion wave that it is not seen and so weakens the slow shock that it does not separate.

When the applied current is sufficient to substantially reverse B_θ at the interface, a structure typified by the oscillogram of Fig.3 is seen by a magnetic probe positioned at $z = 0.14$ m, $r = 0.145$ m. The general structure is as predicted in Fig.2(b). The broad region of decreasing B_θ we identify as the fast expansion wave. This is followed by a short plateau region and then a sharp decrease in B_θ to

almost zero. This latter we identify as a slow, almost switch-off, shock. Behind the shock is another plateau before B_{θ} increases in the opposite direction in what we identify with the piston. This pattern was found for $0.11 \text{ m} < r < 0.18 \text{ m}$ (outside this range axial currents modify the flow) and for propagation up to $z = 0.20 \text{ m}$, corresponding to the end of the applied current pulse. The shock is almost planar while the piston tilts slightly back at larger radii. The features separate with time as is shown by the measured velocities quoted below.

COMPARISON WITH THEORY

Although B_{θ} varies with radius we can compare theory with experiment at the particular radius and conditions appropriate to Fig.3, i.e., $r = 0.14 \text{ m}$, $z = 0.145 \text{ m}$, $B_{z0} = 0.15 \text{ T}$, $B_{\theta0} = 0.13 \text{ T}$, $n_{e0} = 5 \times 10^{20} \text{ m}^{-3}$, $T_{e0} = 1.3 \text{ eV}$.

The boundary conditions for the theory are provided by the measured piston velocity $V_p = 80 \text{ km/s}$ and the measured transverse field in front of the piston, that is behind the shock, $B_{\theta2} = 0.02 \text{ T}$. The predictions of the theory for this case are shown in Fig.2b.

We are able to make direct comparison between theory and experiment for the following parameters: velocities of (i) the front of the expansion wave $V_E = c_{f0}$ and (ii) the shock in the laboratory frame V_s , and the change in transverse field across (i) the expansion wave $\delta B_{\theta E}$, and (ii) the shock $\delta B_{\theta S}$. Good

agreement is obtained as shown in the table:-

	Expt.	Theory
V_E (km/s)	180	194
V_S (km/s)	120	121
$\delta B_{\theta E}$ (T)	-0.03	-0.033
δB_{θ} (T)	-0.08	-0.077

The conditions in front of the shock wave, obtained through the measured expansion $\delta B_{\theta E}$, are plasma velocity $V_{z1} = -20$ km/s (towards shock), $c_{s1} = 16.5$ km/s, $c_{i1} = 154$ km/s and $c_{f1} \approx c_{fo}$. Hence the velocity of the shock relative to the plasma $u_1 = V_S - V_{z1} = 140$ km/s and the corresponding Mach number $M_s = u_1/c_{s1} = 8.5$. The shock clearly satisfies the condition $c_{s1} < u_1 < c_{i1} < c_{f1}$ for a slow shock.

We have therefore produced a slow mode shock wave and verified a model of the launching process.

We thank Dr. R. J. Bickerton for his advice and Mr. L. S. Holmes for his assistance.

REFERENCES

1. J. W. M. Paul et al., Nature 208, 133 (1965).
2. A. D. Craig and J. W. M. Paul, J. Plasma Phys. (Accepted for publication) (Culham Laboratory Preprint CLM-P318).
3. A. E. Robson and J. Sheffield, Third International Conference on Plasma Physics and Controlled Nuclear Fusion Novosibirsk, (1968). Proceedings IAEA, Vienna, 1969, Vol. 1, pp 119-128.
4. A. Kantrowitz and H. E. Petschek, "Plasma Physics in Theory and Application", W. B. Kunkel, ed. (McGraw-Hill Book Company, Inc., N.Y., 1966).
5. J. W. Chao and S. Olbert, J. Geophys. Res. 75, 6394 (1970).
6. L. F. Burlagu and J. K. Chao, J. Geophys. Res. 76, 7516 (1971).

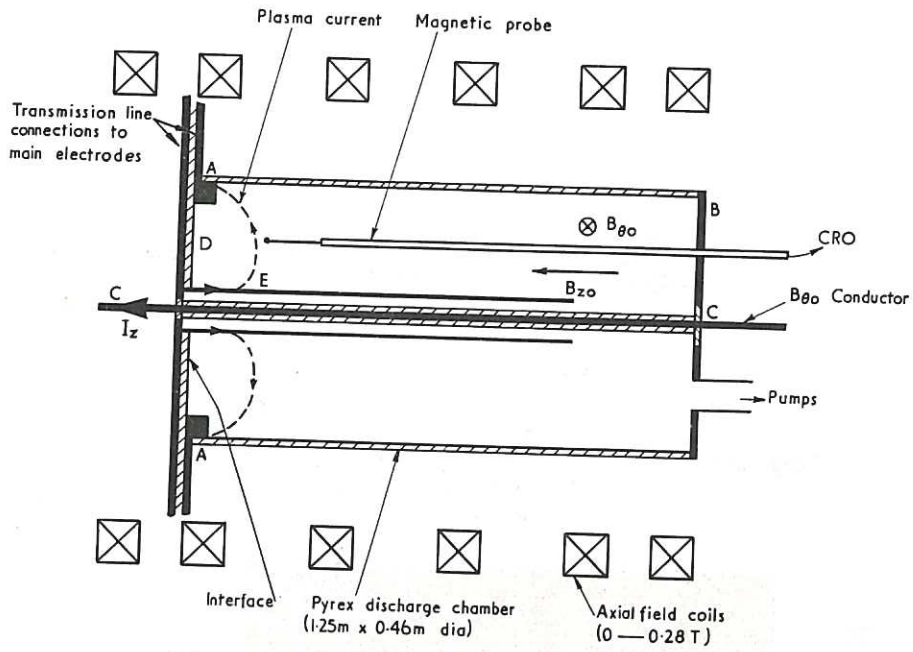


Fig. 1 Schematic of the apparatus

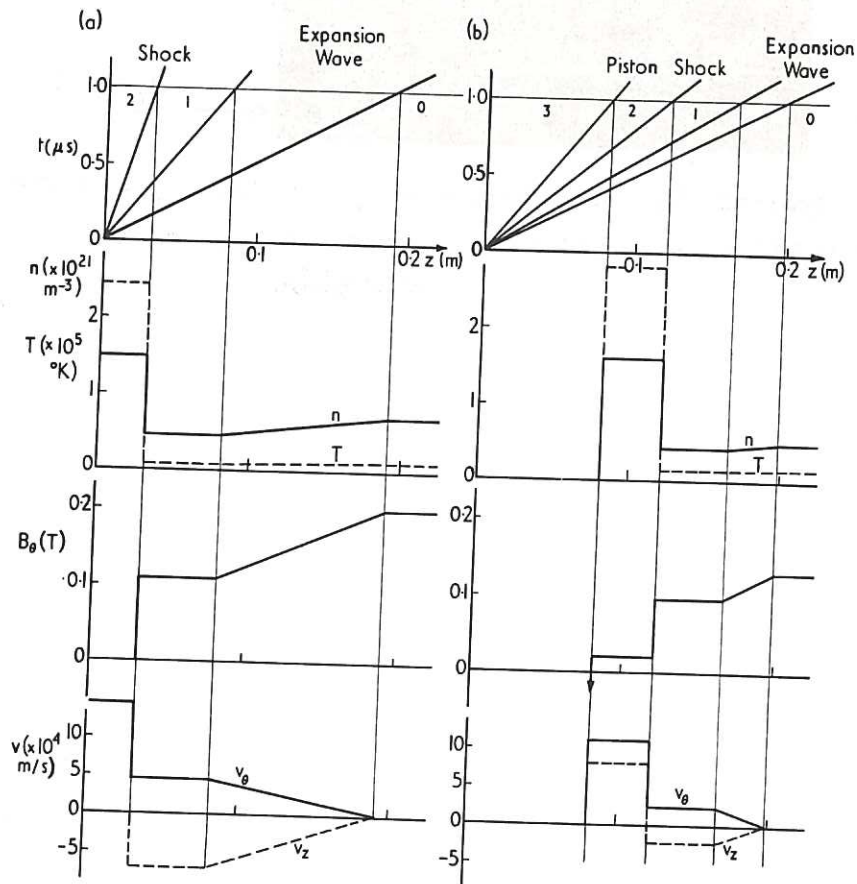


Fig. 2 Theoretical Flow Patterns

- (a) Idealised case neglecting viscous boundary layer
- (b) Finite piston velocity included

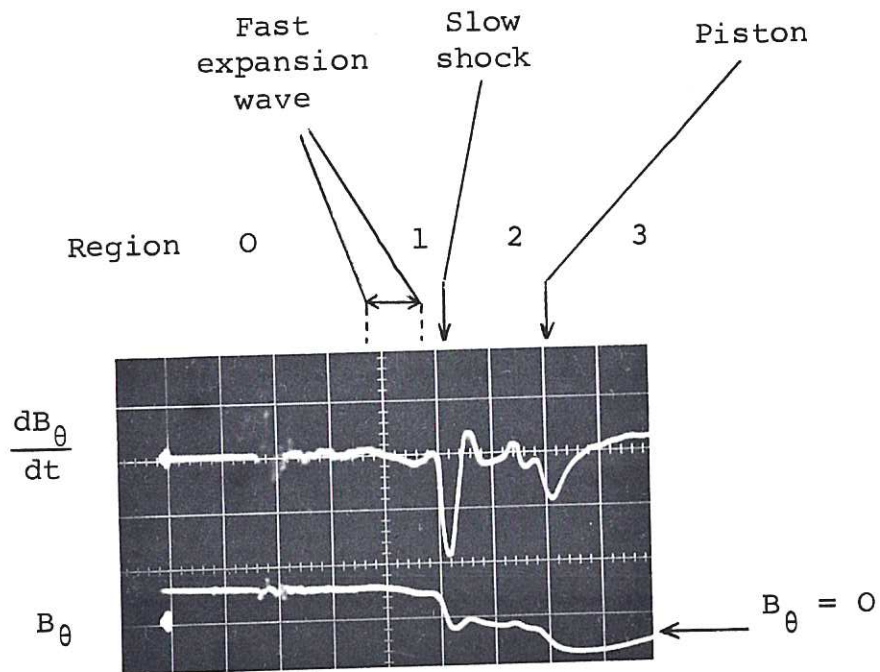


Fig. 3 Typical B_{θ} oscillogram ($B_{z0} = 0.15T$, $B_{\theta0} = 0.13T$,
 $r = 0.142$ m, $z = 0.14$ m, time base = $0.5 \mu\text{sec/div}$)



